HHS Public Access

Author manuscript

Ann Biomed Eng. Author manuscript; available in PMC 2017 October 01.

Published in final edited form as:

Ann Biomed Eng. 2016 October ; 44(10): 2984–2993. doi:10.1007/s10439-016-1636-0.

Swelling of Collagen-Hyaluronic Acid Co-Gels: An *In Vitro* Residual Stress Model

Victor K. Lai[1], **David S. Nedrelow**[2], **Spencer P. Lake**[3], **Bumjun Kim**[2], **Emily M. Weiss**[2], **Robert T. Tranquillo**[2,4], and **Victor H. Barocas**[2,*]

[1]Department of Chemical Engineering, University of Minnesota – Duluth

[2]Department of Biomedical Engineering, University of Minnesota – Twin Cities

[3]Department of Mechanical Engineering & Materials Science, Washington University in St. Louis

[4]Department of Chemical Engineering and Materials Science, University of Minnesota

Abstract

Tissue-equivalents (TEs), simple model tissues with tunable properties, have been used to explore many features of biological soft tissues. Absent in most formulations however, is the residual stress that arises due to interactions among components with different unloaded levels of stress, which has an important functional role in many biological tissues. To create a pre-stressed model system, co-gels were fabricated from a combination of hyaluronic acid (HA) and reconstituted Type-I collagen (Col). When placed in solutions of varying osmolarity, HA-Col co-gels swell as the HA imbibes water, which in turn stretches (and stresses) the collagen network. In this way, co-gels with residual stress (i.e., collagen fibers in tension and HA in compression) were fabricated. When the three gel types tested here were immersed in hypotonic solutions, pure HA gels swelled the most, followed by HA-Col co-gels; no swelling was observed in pure collagen gels. The greatest swelling rates and swelling ratios occurred in the lowest salt concentration solutions. Tension on the collagen component of HA-Col co-gels was calculated from a stress balance and increased nonlinearly as swelling increased. The swelling experiment results were in good agreement with the stress predicted by a fibril network + non-fibrillar interstitial matrix computational model.

KEY TERMS

Multiscale; Pre-Stress; Biomechanics; Donnan; Osmotic; Tissue; Network; Fiber

INTRODUCTION

Tissue-equivalents (TEs), which are simple model tissues with tunable properties, have been used for decades to explore many features of soft tissues, such as how structural and compositional properties affect mechanical function[8]. For example, the relationship between

*Corresponding Author: Victor Barocas, 7-105 Nils Hasselmo Hall, 312 Church St. SE, Minneapolis, MN 55455, baroc001@umn.edu, phone: 612-626-5572, Fax: 612-626-6583.

There are no conflicts of interest.

microscopic fiber alignment and macroscopic mechanical properties has been studied extensively in this model system[16, 36, 22, 20, 26]. Collagen gels, often in conjunction with other biopolymers, have served for a long time as the basis for many engineered tissues[39]. Also, collagen gels, fibrin gels, and/or collagen-fibrin co-gels have been studied in terms of (1) ultimate tensile strength[34], (2) network mechanics[19, 33] and architecture[18], and (3) microstructure and mechanics after selective digestion of one component[18]. Collagen and HA Co-Gel microstructures were previously examined along with mechanical failure, and viscoelasticity[17].

To the best of our knowledge, one aspect not captured in previous TE formulations is residual stress due to interactions among components with different mechanical rest states, which has an important functional role in many tissues[31] (e.g., blood vessels[23], articular cartilage[14, 35], ligaments[40], and annulus fibrosus[27]). Other studies aimed at developing engineered materials that exhibit residual stress behaviors observed in nature have previously been published[5, 32, 30], but unlike our HA-Col co-gels, these materials do not attempt to model residual stress in soft collagenous tissues. Since the resting stress state of native tissues is not easily replicated in TE fabrication, a different method for pre-stressing collagen networks of TEs was necessary.

Hyaluronic Acid (HA) is a linear disaccharide glycosaminoglycan found in various connective, epithelial, and neural tissues. It has been suggested that HA plays a role in various biological processes, such as lubrication in articular cartilage[24], inflammation[11], metastasis, tumor development, migration, mitosis, and wound healing[3]. HA gels are a versatile biomaterial that can be tuned conveniently in terms of both rheological and mechanical/physical properties with its concentration or molecular weight and can encapsulate cell-signaling chemokines, or even viable cells[9]. Its inherent advantages of biocompatibility and the ability to elicit desirable cellular responses such as proliferation, and migration have made it a popular base for tissue engineering[13], and drug delivery[25]. Use of soluble HA on its own, however, is limited by low mechanical strength and rapid degradation, so HA is often chemically cross-linked[41, 37] and/or co-gelated with other extra-cellular matrix molecules such as collagen[4, 39, 17].

With one charged carboxylate group for each disaccharide monomer[41, 15], HA is a semi-rigid polyelectrolyte that possesses a high fixed charge density. When HA is placed in aqueous solution, an osmotic pressure develops within the gel via the Donnan effect[10]. The amount of Donnan-osmotic swelling decreases the ionic concentration of the solution. Collagen gels, in contrast, exhibit no significant swelling over a wide range of solution osmolarities.

The current work exploited the difference in swelling properties between collagen and HA gels to create a pre-stressed model tissue system. When a collagen-HA co-gel is fabricated, it is assumed that both components are stress-free and at the same gel volume. When a hypo-osmotic challenge is introduced, the equilibrium state of the HA is swelled due to the Donnan effect, but the equilibrium state of the collagen is unchanged because collagen does not swell appreciably. As a result, the new gel has two components with two different equilibrium states, and the externally unloaded state of the gel is one in which collagen

tension and HA compression cancel out to produce a net stress of zero. The goals of the present study were to fabricate HA-Col co-gels, measure their swelling properties, quantify the amount of pre-stress introduced to the collagen network, and compare the results to a computational network simulation.

MATERIALS AND METHODS

Sample Fabrication

Three groups of gels were fabricated: (1) Col, (2) HA, and (3) HA-Col co-gels. For collagen, reconstituted Type-I rat tail collagen (Invitrogen, Carlsbad, CA) was mixed as described previously with 1M HEPES, 1M NaOH, 10X MEM, FBS, Penicillin/Streptomycin, Fungizone, and L-Glutamine, and diluted with deionized, distilled water to a final concentration of 1 mg/ml[19]. HA samples were prepared by mixing thiol-modified HA (Biotime, Inc., Alameda, CA) with a polyethylene-glycol-based thiol-reactive cross-linker to form a 0.67% (w/v) HA gel (240 +/− 20 kDa). The HA monomer was heterogenous with approximately 60% HA, and 40% thiol-modified HA. HA-col co-gels were prepared by mixing equal volumes of Col and HA (with cross-linker) solutions, such that final concentrations for each component were consistent with the single-component gels. After the solutions had been made, 10-μL aliquots of each gel type were cast in silicone oil and incubated at 37°C for 24 hours to create spheres of ~2.5 mm diameter, similar to a previously reported procedure[28].

Swelling Experiments

After incubation, HA-Col co-gel spheres were placed in solutions of 0, 1, 2, 3, 4, 5, 10, 15, 25, 50, 75 or 100%, and Pure HA gel spheres were placed in 0, 0.5, 1, 2, 5, 10, 15, 20, 25, 50, 75, 100% 1x Dulbecco's phosphate buffered saline (PBS, Corning Inc., Corning, NY, dilute with deionized, distilled water, n = 3–4 per solution). The gels were then allowed to swell for 2 hours, with images captured every 2 minutes on a Leica S6D dissecting microscope (Leica Camera AG, Wetzlar, Germany) affixed with a 1.3 megapixel digital camera and image-capturing software (Motic China Group Co., Ltd., Hong Kong, P.R. China). Sphere diameters were computed either (1) by a custom Matlab routine (DOI 10.5281/zenodo.44285) that image-segmented each image, recorded the signal area, and returned gel diameters for each image; or (2) for those gels that were highly translucent, as the average of 2 orthogonal directions measured manually. The equilibrium diameter (D_{eq}), and the initial (D_o) diameter of the gels were recorded for further steady-state analysis. An exponential curve was fit to the data (Fig. 1) to calculate both the equilibrium swelling ratio (D_{eq}/D_o), and the characteristic swelling time $\tau = (1/k)$ for each sample. See figure 1.

Data Analysis

The fixed-charge density of HA before swelling, c_F^0, was estimated by

$$c_F^0 = \frac{|z_{HA}|C_{HA}}{MW_{HA}} \quad (1)$$

where z_{HA} was the charge per HA monomer, C_{HA} was the mass concentration of HA, and MW_{HA} was the molecular weight of an HA disaccharide monomer. For an HA concentration of 6.67mg/mL, with $|z_{HA}|$ = 0.61 and MW_{HA} = 60% (HA: 379 g/mol) + 40% (HA-Thiol: 478 g/mol), $c_F^0 \cong 9.7$ mM. It was assumed that all of the thiolates had the same pK_a of 8.87, whether they cross-linked or not[41], and that all of the carboxylates in HA were dissociated (pK_a= 3–4). The fraction of charged monomers was determined with the Henderson-Hasselbalch equation and a solution pH of 7.4. The superscript '0' indicated the fixed charged density of an unswelled HA gel. Since the HA gels were dilute (0.667% w/v), the fixed charge density after swelling, c_F, was calculated by

$$c_F = c_F^{\,0} \left(\frac{D_0}{D}\right)^3 \quad (2)$$

where D_0 and D were the diameters of the HA sphere before and after swelling, respectively.

For an HA gel immersed in a solution dominated by monovalent ions (e.g., NaCl) the Donnan osmotic pressure, π_{Donnan}, can be computed as[10]

$$\pi_{Donnan} = RT\Delta c = RT\left(\sqrt{c_F^{\,2} + 4c^{*2}} - 2c^*\right) \quad (3)$$

where R is the universal gas constant, T is the absolute temperature of the system, and c^* is the concentration of Na^+ ions in the external solution, assuming complete ionization and ideal solution behavior. For a swollen HA gel at equilibrium, the Donnan osmotic pressure is balanced by the hydrostatic stress in the HA gel, σ_{HA}:

$$\sigma_{HA} - \pi_{Donnan} = 0 \quad (4)$$

Similarly, a swollen HA-Col gel at equilibrium, under the assumption that the co-gel obeys constrained mixture theory[29, 7], satisfies the following stress balance:

$$\Phi_{HA}\sigma_{HA} + \sigma_{Col} - \pi_{Donnan} = 0 \quad (5)$$

where Φ_{HA} = 0.99, the volume fraction of HA in HA-Col co-gels, σ_{Col} is the Cauchy stress in the collagen network, and π_{Donnan} is calculated using Eq. 3.

The above equations, together with the results of the swelling experiments, were used to calculate each stress component of equation 5 (σ_{HA}, π_{Donnan}, and σ_{Col}) for the HA-Col co-gel at equilibrium. As described above, tension was generated in the collagen during swelling, but it could not be measured directly. Collagen stress was calculated after measuring the other components and solving the stress balance (Eq. 5) for swollen HA-Col co-gels. Solving for collagen stress in the co-gel was completed as follows. First, a swelling

experiment on pure HA provided a swelling ratio, D_o / D. Together with the known salt solution concentration, the swelling ratio was used to solve equation 2. Once c_F had been calculated, the salt concentration, c^*, was entered into equation 3 to compute the Donnan osmotic pressure, π_{Donnan}. In the pure HA gel, the Donnan pressure was equal to σ_{HA}, the HA stress (Eq. 4), which was then plotted against the swelling ratio and fitted to obtain equation 6.

$$\sigma_{HA} = 0.945\, ln\left(\frac{D}{D_0}\right)^3 \quad (6)$$

Where the constant, 0.945 was obtained from the fit to pure HA swelling data plotted in figure 4A.

Under the assumption that the relationship between swelling and HA stress in pure HA gels was similar to that in HA-col co-gels, equation 6 was used to approximate σ_{HA} in swollen co-gels. For consistency, minor differences in stress behavior between pure HA and HA in the co-gels were accounted for with a volume fraction of HA introduced in Eq. 5. Again, Eq. 3 was used as above to find π_{Donnan} in HA-Col co-gels, leaving σ_{Col}, as the only remaining unknown in Eq. 5. Swelling experiment data were analyzed and plotted in terms of: Swelling ratio = D/Do, characteristic swelling time τ = 1/k, and initial swelling rate = (Deq/Do − 1) / τ.

Statistical Analysis

All error bars in the figures are 95% confidence intervals. The number of replicates varied between experiments with a minimum of 6 and a maximum of 12 samples. One-way ANOVA was applied to HA's characteristic swelling time (Fig. 3B), and applied to initial swelling rate results (Fig. 3C) with statistical software R. Because high concentration PBS had little swelling effect on the samples, the reference group was defined to be 100% PBS. The null hypothesis stated that the mean of the measurements for a given concentration was the same as the mean of the measurments from the 100% PBS experiment. There were ten different independent comparisons (one for each experimental concentration of PBS), so a Bonferroni correction was used to correct for the overall type I error. The Bonferroni corrected significance level was 0.005 ($\alpha_{bonf} = \alpha / 10$).

Computational Network Model

Experimental results of collagen pre-stress, σ_{Col}, were compared to computational model predictions using our microscale network model as described previously[21, 36]. Briefly, a representative volume element (RVE) containing a Voronoi network of randomly oriented fibers was generated, where fibers were connected to one another, as well as to the RVE boundaries, via crosslinks represented by freely-rotating pin-joints. The mechanical response of each fiber within the network was governed by the non-linear force-strain constitutive equation

$$F=\frac{A}{B}[\exp(BE_f)-1] \quad (7)$$

where F is the force exerted by the individual fiber, and A and B are material parameters that characterize the mechanical behavior of the fiber. E_f is the Green strain of each fiber, calculated from the fiber stretch, λ:

$$E_f=0.5(\lambda^2-1) \quad (8)$$

As the RVE is deformed, the average Cauchy stress in the network, $<\sigma_{ij}>$, is given by the sum over boundary crosslinks as

$$\langle\sigma_{ij}\rangle=\frac{1}{V}\sum x_i F_j \quad (9)$$

where V is the volume of the RVE, x_i is the *ith* component of the nodal position of a boundary crosslink, and F_j is the *jth* component of the fiber force exerted on that boundary crosslink. The RVE is scaled to the known macroscopic scale via a scale factor α, by relating the total fiber length of the RVE network (L) with the known macroscopic collagen volume fraction (θ) and average cross-sectional area of a collagen fiber (A_f):

$$\alpha=\sqrt{\frac{LA_f}{\theta}} \quad (10)$$

From SEM images of acellular collagen gels, an average collagen fiber diameter of 50nm was used, corresponding to $A_f \sim 2{,}000\ nm^2$.

To obtain material parameters A and B for our collagen gels, simulations of uniaxial tensile tests on 5 Voronoi RVE networks were performed, and their stress-strain curves were fitted to experimental tensile test data that had been obtained previously[18]. Using these fitted parameters (A = 30 nN, B = 4) as inputs for our computational model, purely dilatational stretches of 5 different Voronoi network computations were performed to simulate swelling which was driven by the nonfibrillar matrix, HA. The nonfibrillar matrix and fibrillar network were coupled in that they had the same displacement at all points as in constrained mixture theory.[38] The average stress predicted by 3-D network stretches was then compared with σ_{Col} obtained from HA-Col co-gel swelling experiments.

RESULTS

Swelling occurred only in the pure HA and HA-Col gels. Figure 2 shows representative swelling behavior exhibited by individual spheres immersed in 0%vol PBS (pure deionized,

distilled water). Swelling ratio D/D_o vs. time was plotted for the three gel types (Fig. 2B). Pure collagen gels did not swell appreciably over 1 hour, and no further data were logged. The pure HA gel, in contrast, swelled the fastest and to the highest degree, as demonstrated by the steep initial slope and large equilibrium swelling ratio. The HA-col co-gel sphere also exhibited swelling, but not as rapidly as, nor to as great an extent as the pure HA gel. Pure collagen gels did not swell in any of the solutions, but HA and HA-Col gels had clear changes in swelling behavior with changes in the PBS level in the medium (Fig. 3A). As expected from the theoretical analysis, the swelling ratio decreased with increasing PBS concentration for both HA and HA-Col co-gels, with the largest decrease occurring in the lower concentrations of PBS from 0%vol to 25%vol PBS. Comparison of characteristic swelling times (Fig. 3B), showed that the HA-Col gels exhibited a decreasing trend in characteristic swell time, with increasing PBS concentration. For the HA gels, however, those in 0%vol PBS showed the shortest characteristic swelling time, followed by a rise to a maximum swell time and then a drop in swell time for high PBS levels. For HA, the experimental groups with PBS concentrations between 1% and 25%vol PBS were statistically different from 100%vol PBS. This result, coupled with the largest swelling ratio for the pure HA gels in 0%vol PBS, meant that these gels had a very fast swelling rate. The initial swelling rate for HA-Col co-gels decreased with increasing PBS concentrations up to 10%, and then remained roughly constant (Fig. 3C).

The stress in pure HA gels was found to be roughly logarithmic with the swelling ratio (Fig 4A), in spite of considerable scatter in the data. Using the regression line for pure HA swelling data in figure 4A, σ_{HA} was estimated for the HA-Col co-gels, and the collagen stress in the swollen gel, σ_{Col} was calculated using equation 5. The relative magnitude of each stress contribution is shown in Figure 4B. The calculated stress induced in the collagen network increased nonlinearly with swelling, opposing the Donnan pressure. For the HA-Col co-gels that exhibited the largest swelling ratio (i.e., those immersed in 0%vol PBS), the collagen contribution was 85% of the Donnan stress, and the HA contribution was 15%. The linear stretch exerted on the collagen network under those conditions (stretch (D/D_0) = 1.49 +/− 0.07) was slightly larger than the average stretch at failure of ~1.39 +/− 0.04 for pure collagen gels of the same concentration under uniaxial stretch[18].

Dilatational stretch simulations of pure collagen gels (Fig. 5A) computed collagen stresses similar to those observed in HA-Col co-gel swelling experiments (Fig. 5B). The data points that lie at the lower stretch ratios on the x-axis corresponded to higher PBS concentrations.

DISCUSSION

The primary goal of this study was to explore the mechanics of HA-Col co-gels as an *in vitro* system as a model of residual stress in biological tissues. As expected, pure HA swelled in hypo-osmotic solution, but Col did not. When fabricated in a co-gel, HA-Col exhibited intermediate swelling behavior which suggested that this system possessed residual stress. The tension of the collagen fibril network in swelled HA-Col spheres was quantitated by solving a stress balance composed of: (1) the Donnan osmotic pressure, (2) HA Cauchy stress, and (3) Col Cauchy stress. The Donnan osmotic pressure that drives swelling in HA was calculated from known PBS concentrations and charge density of HA,

and the HA stress was estimated from a fit to pure HA swelling data. No mechanical interactions between collagen and HA were considered in the stress balance, and yet collagen stresses in swollen co-gels were found to be in good agreement with an independent prediction generated by a fibrillar-network computational simulation, with the swelling effect simulated as a triaxial extension on the fibrillar network. Thus the simulation recapitulated the co-gel's collagen stresses as a model that accounted for both the fibrillar network and non-fibrillar matrix.

It was previously observed that both failure stress and failure strain during unconfined compression of HA-Col Co-gels increased with increasing HA content[17]. This observation suggests HA has a dramatic effect on the co-gel system in the high stress and strain regimes during compression, but little is known about the underlying mechanism. The current study did not examine failure, but estimates of each component stress may provide some insight about the co-gel's mechanical response both at failure and at the lower strains examined here. More of the load was supported by collagen tension (85% in 0%vol PBS), but HA did support nearly 1/6 of the load (15%) (Fig. 4B). Conceptually, the collagen network may be ultimately responsible for co-gel integrity, and the significant proportion of the load absorbed by HA may provide collagen some support resulting in higher failure stresses for HA-Col co-gels than for pure Col gels. Large stretches that exceeded the failure stretch of pure Col gels were observed in intact co-gels swollen in water (1.49 vs. 1.39 for pure col failure). Assuming that failure is caused by compromising the collagen network, and not HA, these highly stretched yet intact swollen co-gels suggest agreement with the notion that HA-col co-gels have a higher failure strain than pure Col in uniaxial tension. The stretches above compared pure Col in uniaxial tension, but HA-Col swelled in three dimensions, which was suggested to have a different effect on the amount of stretch exhibited by individual fibrils within the network[36]. Further studies with different HA-Col formulations and/or modes of mechanical loading might be able to determine whether the HA-Col co-gel response includes additional interactions between its material components.

It was previously suggested that introducing relatively small amounts of HA to co-gels has little effect on the collagen fibril dimensions[17]. The mechanics of the co-gels in that study were altered by the presence of HA, where more HA exhibited greater compressive resistance and were more viscous-fluid in nature (reduced storage modulus, G'). No microstructural characterizations were carried out in the present work, but the characteristic swelling times and equilibrium swelling ratios were quantified (Fig. 3A, B). Pure HA required a longer period of time to swell to equilibrium than HA-Col co-gels in all PBS concentrations except 0%. The fast swelling time for pure HA in 0% PBS raises an interesting question as to whether or not the polymer hydrodynamics were altered at the highest osmotic-pressure-driven fluid velocity[2, 12]. For PBS concentrations from 1% to 25%vol, HA gels exhibited a characteristic swelling time that was significantly longer than that observed in 100%vol PBS. In all of the observed concentrations except 0% PBS, HA's characteristic swelling time was longer than HA-Col co-gels. HA-Col co-gels exhibited approximately constant characteristic swelling times across the lower PBS levels, but above 15%, the times decreased (fig. 3B). The swelling size was less for those co-gels immersed in the high PBS regime (> 15%). The initial swelling rate decreased, but then remained constant for the high PBS regime (Fig 3C). Taken together, the decreasing trends in

characteristic swelling time and swollen size, along with constant initial rate suggest there is a different swelling mechanism for HA-Col in the low vs. the high PBS concentration regime. The dynamic mechanism of swelling that involves diffusion and water movement was beyond the scope of this study, but would be of significant interest in further research analyzing HA-Col co-gel swelling behavior[1], perhaps through the use of multiphasic mixture theory[6], of the mechanism underlying the results observed here.

The viscoelastic relaxation time of articular cartilage, when modeled with polymer reptation theory, was suggested to be proportional to the applied osmotic pressure raised to the 3/2 power[35]. This theoretical relationship was not observed in our experimental data, but changing characteristic swelling times were observed at high PBS levels (Fig 3B). One of Ruberti and Sokoloff's assumptions in the reptation analysis was that the articular cartilage is highly compressed, so the osmotic pressure due to the counter-ion force dominates over the contribution to osmotic pressure made by the HA monomer. That assumption may not apply to our swelled gels.

For the pure HA gels, the walls of the spheres were nearly undetectable, so those gels were hand-measured, introducing greater variability than was present for the HA-Col co-gels and pure Col gels measured with an automated Matlab routine (Fig. 2B). Such measurement variability may have been responsible in part for the deviation of Pure HA data from the regression line in Fig. 4A. Another possible source of error may have been gel inhomogeneity, as the distributions of either HA or Col throughout the sphere could have been irregular, leading to variations in swelling. In spite of the potential sources of both measurement and material error, the data had a small standard deviation of 0.08 for 8 samples (5% of equilibrium swelling ratio) of pure HA in 0%vol PBS and this was a smaller standard deviation than was observed in any other experimental group. Also, the average monomer charge, $z_{HA} = 0.61$, for HA in the gels was approximated from the dominant functional group in each of the monomer types, where the pKa of carboxylate determined the charge dissociation for HA and that of thiolate for thiol-modified HA. The actual fixed charge density in HA-col co-gel was likely different from this theoretical calculation, introducing error to the stresses reported here.

Independent estimates of the collagen stress based on (1) swelling experiments and (2) a computational network model based on uniaxial extension of pure Col gels showed good agreement over the experimental range (Fig. 5B). In Sander et al. 2009, biaxial extension of the gel caused the fibrils to exhibit nearly affine kinematics – especially at high strains – but a uniaxial stretch resulted in average fibrils stretches much less than that of the overall network. In the uniaxial fitting process used here, it was assumed that the fibrils in the network simulation were strained in a manner consistent with that of the pure collagen gel. The same material parameters were then used in triaxial extension to predict the stresses generated by swelled HA-Col co-gels, where the network behavior was expected to be almost perfectly affine by virtue of triaxial homogenous loading. Because there was still good agreement with swelling data (Fig. 5B), we conclude that the network kinematics in the simulation are roughly representative of the collagen's in swelling experiments.

The agreement between simulation and experiment was not, however, perfect. The triaxial extension simulation underestimated experimental stress at low strains, and overestimated the stress at high strains. That difference could be due to HA restricting the conformational space available to collagen network fibrils, particularly in the low strain regime, suggesting an interaction between the HA and the collagen that would further drive the system toward affinity (Fig. 5B). Such a response was observed previously in collagen-agarose co-gels[20], where the measured strength of collagen fibril alignment (retardation) during uniaxial loading was lessened in the presence of agarose, representing inhibition of the collagen network's microstructural reorganization. The differences between experiment and simulation appear to be diminished at increased strain. The triaxial extension simulation necessarily exhibited affine kinematics over the strain range tested, but the co-gel microstructure was not characterized. Therefore, non-affine kinematics is one potential explanation for the disagreement between simulation and experiment, but the experiments were swelled in three-dimensions, implying this too would be highly affine. Material inhomogeneity, where the spatial origins of swelling were displaced from the center of the sphere, is a possible reason for the different stresses at low strain that would be overcome at high strain. Regardless of the mechanism, the experiment and simulation stresses computed here at steady-state were similar in scale. In addition, the successful use of pure HA to estimate σ_{HA} in co-gels suggests that mechanical interactions between HA and collagen in the co-gel may have negligible mechanical consequences in swelling.

The simple, *in vitro* HA-Col co-gel model is a candidate system to approximate the residual stresses commonly observed in living tissues. HA-Col co-gels exhibited residual stress behavior when swelled in a wide range of PBS concentrations. A computational simulation of a fibril-network + non-fibrillar interstitial matrix model generated stresses similar to those of the collagen component of swelled HA-Col co-gels, implying mechanical interaction terms between the HA and collagen components may be considered negligible. Further study of this *in vitro* system could enhance our present understanding of failure, non-affine behavior, and HA's influence on collagen network microstructures in a way that more closely approximates the complexity of a wide range of biomechanical behaviors *in vivo.*

Acknowledgments

This work was supported by the National Instutute of Health (RO1 EB005813), and by a resources grant from the Minnesota Supercomputing Institute.

References

1. Albro MB, Chahine NO, Caligaris M, Wei VI, Ng KW, Hung CT, Ateshian GA. NIH Public Access. 2010; 129:503–510.
2. Alexander-Katz, a; Netz, RR. Dynamics and instabilities of collapsed polymers in shear flow. Macromolecules. 2008; 41:3363–3374.
3. Alexander A, Donoff RB. of Open Wounds1. 1980; 429:422–429.
4. Anandagoda N, Ezra DG, Cheema U, Bailly M, Brown RA. Hyaluronan hydration generates three-dimensional meso-scale structure in engineered collagen tissues. J R Soc Interface. 2012; 9:2680–7. [PubMed: 22593098]
5. Armon S, Efrati E, Kupferman R, Sharon E. Geometry and Mechanics in the Opening of Chiral Seed Pods. Science. 2011; 333:1726–1729. [PubMed: 21940888]

6. Ateshian GA, Maas S, Weiss JA. Multiphasic finite element framework for modeling hydrated mixtures with multiple neutral and charged solutes. J Biomech Eng. 2013; 135:111001. [PubMed: 23775399]
7. Barocas VH, Tranquillo RT. An Anisotropic Biphasic Theory of Tissue-Equivalent Mechanics: The Interplay Among Cell Traction, Fibrillar Network Deformation, Fibril Alignment, and Cell Contact Guidance. J Biomech Eng. 1997; 119:137. [PubMed: 9168388]
8. Bell E, Ivarsson B, Merrill C. Production of a tissue-like structure by contraction of collagen lattices by human fibroblasts of different proliferative potential in vitro. Proc Natl Acad Sci U S A. 1979; 76:1274–1278. [PubMed: 286310]
9. Choh SY, Cross D, Wang C. Facile synthesis and characterization of disulfide-cross-linked hyaluronic acid hydrogels for protein delivery and cell encapsulation. Biomacromolecules. 2011; 12:1126–1136. [PubMed: 21384907]
10. Donnan FG. The Theory of Membrane Equilibria. Chem Rev. 1924; 1:73–90.
11. Frey H, Schroeder N, Manon-Jensen T, Iozzo RV, Schaefer L. Biological interplay between proteoglycans and their innate immune receptors in inflammation. FEBS J. 2013; 280:2165–2179. [PubMed: 23350913]
12. Fyhrie DP, Barone JR. Polymer dynamics as a mechanistic model for the flow-independent viscoelasticity of cartilage. J Biomech Eng. 2003; 125:578–584. [PubMed: 14618916]
13. Greco RM, Iocono JA, Ehrlich HP. Hyaluronic acid stimulates human fibroblast proliferation within a collagen matrix. J Cell Physiol. 1998; 177:465–473. [PubMed: 9808154]
14. Han E, Chen SS, Klisch SM, Sah RL. Contribution of proteoglycan osmotic swelling pressure to the compressive properties of articular cartilage. Biophys J. 2011; 101:916–24. [PubMed: 21843483]
15. Hargittai I, Hargittai M. Molecular structure of hyaluronan: an introduction. Struct Chem. 2008; 19:697–717.
16. Jhun CS, Evans MC, Barocas VH, Tranquillo RT. Planar biaxial mechanical behavior of bioartificial tissues possessing prescribed fiber alignment. J Biomech Eng. 2009; 131:081006. [PubMed: 19604018]
17. Kreger ST, Voytik-Harbin SL. Hyaluronan concentration within a 3D collagen matrix modulates matrix viscoelasticity, but not fibroblast response. Matrix Biol. 2009; 28:336–46. [PubMed: 19442729]
18. Lai VK, Frey CR, Kerandi AM, Lake SP, Tranquillo RT, Barocas VH. Microstructural and mechanical differences between digested collagen-fibrin co-gels and pure collagen and fibrin gels. Acta Biomater. 2012; 8:4031–4042. [PubMed: 22828381]
19. Lai VK, Lake SP, Frey CR, Tranquillo RT, Barocas VH. Mechanical Behavior of Collagen-Fibrin Co-Gels Reflects Transition From Series to Parallel Interactions With Increasing Collagen Content. J Biomech Eng. 2012; 134:011004. [PubMed: 22482659]
20. Lake SP V, Barocas H. Mechanical and structural contribution of non-fibrillar matrix in uniaxial tension: A collagen-agarose co-gel model. Ann Biomed Eng. 2011; 39:1891–1903. [PubMed: 21416392]
21. Lake SP, Hadi MF, Lai VK, Barocas VH. Mechanics of a fiber network within a non-fibrillar matrix: Model and comparison with collagen-agarose co-gels. Ann Biomed Eng. 2012; 40:2111–2121. [PubMed: 22565816]
22. Lake SP, Hald ES, Barocas VH. Collagen-agarose co-gels as a model for collagen-matrix interaction in soft tissues subjected to indentation. J Biomed Mater Res A. 2011; 99:507–15. [PubMed: 21913316]
23. Lanir Y. Osmotic swelling and residual stress in cardiovascular tissues. J Biomech. 2012; 45:780–789. [PubMed: 22236524]
24. Laurent, TC. The Chemistry, Biology and Medical Applications of Hyaluronan and Its Derivatives. Portland Press, Limited; 1998. p. 368
25. Luo Y, Kirker KR, Prestwich GD. Cross-linked hyaluronic acid hydrogel films: new biomaterials for drug delivery. J Control Release. 2000; 69:169–84. [PubMed: 11018555]

26. Marquez JP, Genin GM, Pryse KM, Elson EL. Cellular and matrix contributions to tissue construct stiffness increase with cellular concentration. Ann Biomed Eng. 2006; 34:1475–1482. [PubMed: 16874557]
27. Michalek AJ, Gardner-Morse MG, Iatridis JC. Large residual strains are present in the intervertebral disc annulus fibrosus in the unloaded state. J Biomech. 2012; 45:1227–1231. [PubMed: 22342138]
28. Moon AG, Tranquillo RT. Fibroblast-Populated Collagen Microsphere Assay of Cell Traction Force.1. Continuum Model. Aiche J. 1993; 39:163–177.
29. Mow VC, Holmes MH, Michael Lai W. Fluid transport and mechanical properties of articular cartilage: A review. J Biomech. 1984; 17:377–394. [PubMed: 6376512]
30. Nardinocchi P, Pezzulla M. Curled actuated shapes of ionic polymer metal composites strips. J Appl Phys. 2013; 113
31. Nelson D. Experimental Methods for Determining Residual Stresses and Strains in Various Biological Structures. Exp Mech. 2014; 54:695–708.
32. Pan Y, Zhong Z. A nonlinear constitutive model of unidirectional natural fiber reinforced composites considering moisture absorption. J Mech Phys Solids. 2014; 69:132–142.
33. Park SN, Lee HJ, Lee KH, Suh H. Biological characterization of EDC-crosslinked collagen–hyaluronic acid matrix in dermal tissue restoration. Biomaterials. 2003; 24:1631–1641. [PubMed: 12559823]
34. Roeder BA, Kokini K, Sturgis JE, Robinson JP, Voytik-Harbin SL. Tensile Mechanical Properties of Three-Dimensional Type I Collagen Extracellular Matrices With Varied Microstructure. J Biomech Eng. 2002; 124:214. [PubMed: 12002131]
35. Ruberti JW, Sokoloff JB. Theory of the short time mechanical relaxation in articular cartilage. J Biomech Eng. 2011; 133:104504. [PubMed: 22070338]
36. Sander, Ea; Stylianopoulos, T.; Tranquillo, RT.; Barocas, VH. Image-based multiscale modeling predicts tissue-level and network-level fiber reorganization in stretched cell-compacted collagen gels. Proc Natl Acad Sci U S A. 2009; 106:17675–17680. [PubMed: 19805118]
37. Segura T, Anderson BC, Chung PH, Webber RE, Shull KR, Shea LD. Crosslinked hyaluronic acid hydrogels: a strategy to functionalize and pattern. Biomaterials. 2005; 26:359–371. [PubMed: 15275810]
38. Taber, La; Humphrey, JD. Stress-modulated growth, residual stress, and vascular heterogeneity. J Biomech Eng. 2001; 123:528–535. [PubMed: 11783722]
39. Walters BD, Stegemann JP. Strategies for directing the structure and function of three-dimensional collagen biomaterials across length scales. Acta Biomater. 2014; 10:1488–501. [PubMed: 24012608]
40. Weiss JA, Gardiner JC. of Ligament Mechanics. 2001; 29:303–371.
41. Zheng Shu X, Liu Y, Palumbo FS, Luo Y, Prestwich GD. In situ crosslinkable hyaluronan hydrogels for tissue engineering. Biomaterials. 2004; 25:1339–1348. [PubMed: 14643608]

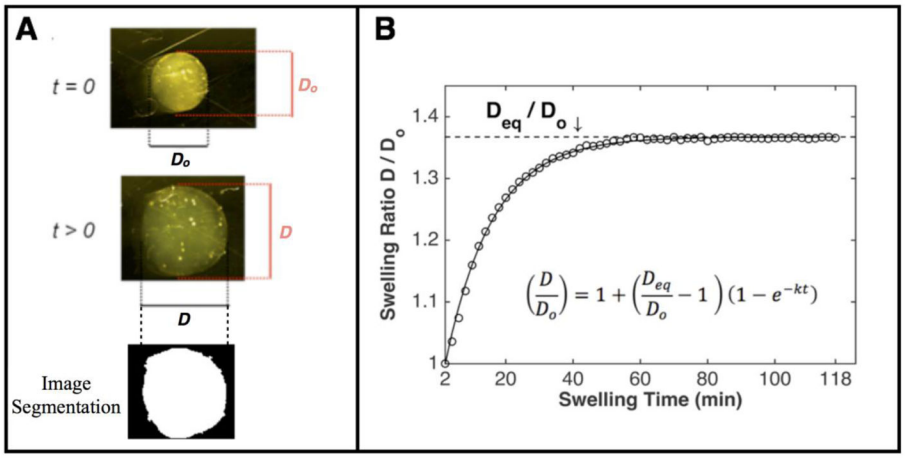

Figure 1.

(A) Gel diameter, *D*, was measured automatically by an image-segmentation Matlab routine from video taken during swelling for 2 hours. B) Example of the exponential curve fit for a gel to experimental data. The fitting parameters were the final swelled equilibrium sphere diameter, D_{eq}, and characteristic swelling time, *1/k.*

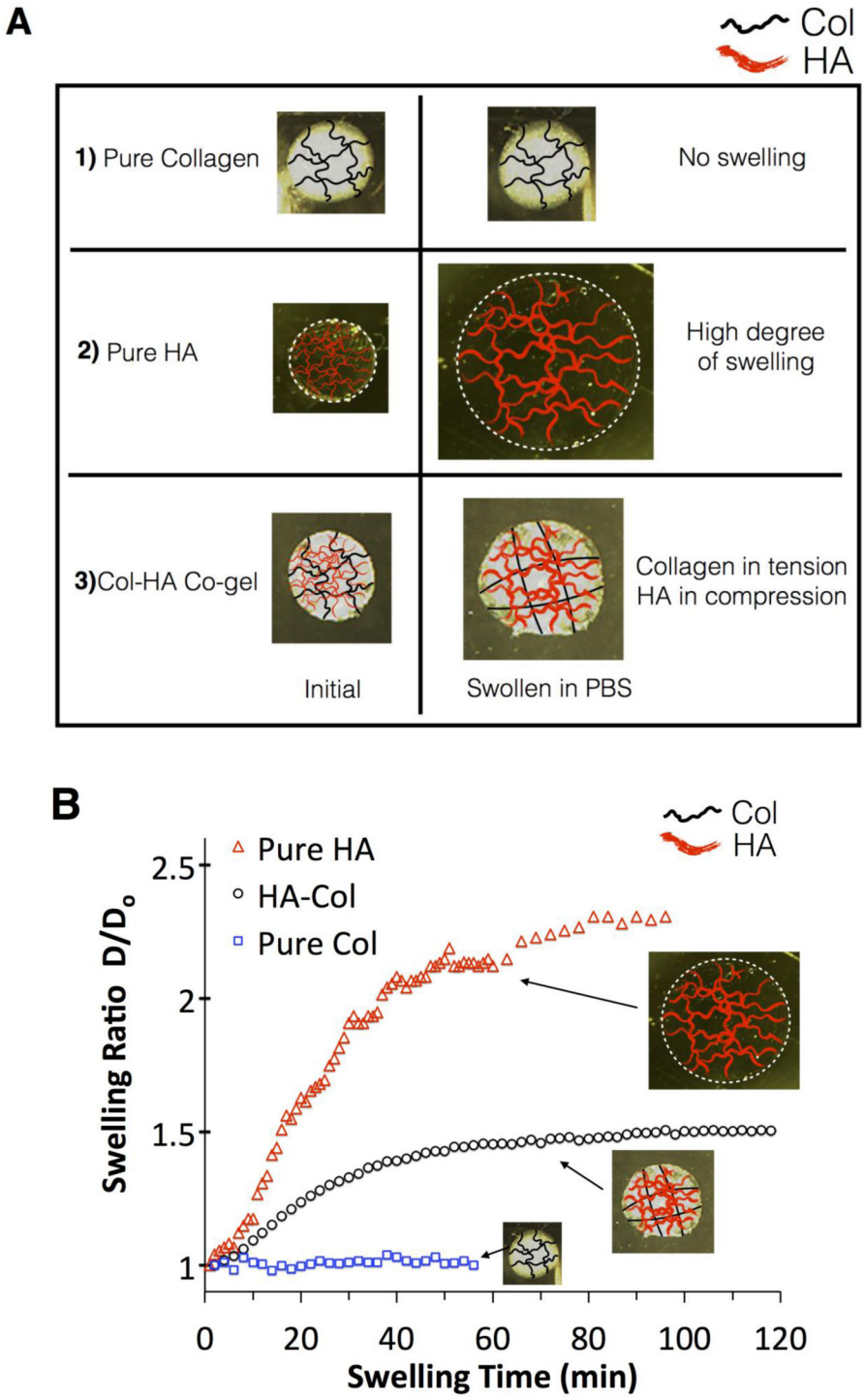

Figure 2.

(A) Three different gel types were studied. Black and red lines in the illustrations are used for demonstration purposes only and were not in the original data. (1) Pure collagen exhibits no swelling, (2) pure HA, with borders encircled, swells to a greater extent, (3) Col-HA co-gels swell to a lesser extent, demonstrating tension in the collagen and compression in the

swelled HA. (B) Individual sphere swelling ratios of each gel type in 0%vol PBS. The greatest swelling in terms of both rate and size increase occurred in pure HA gels. Negligible swelling occurred in pure collagen gels, and intermediate swelling was observed in HA-Col Co-gels.

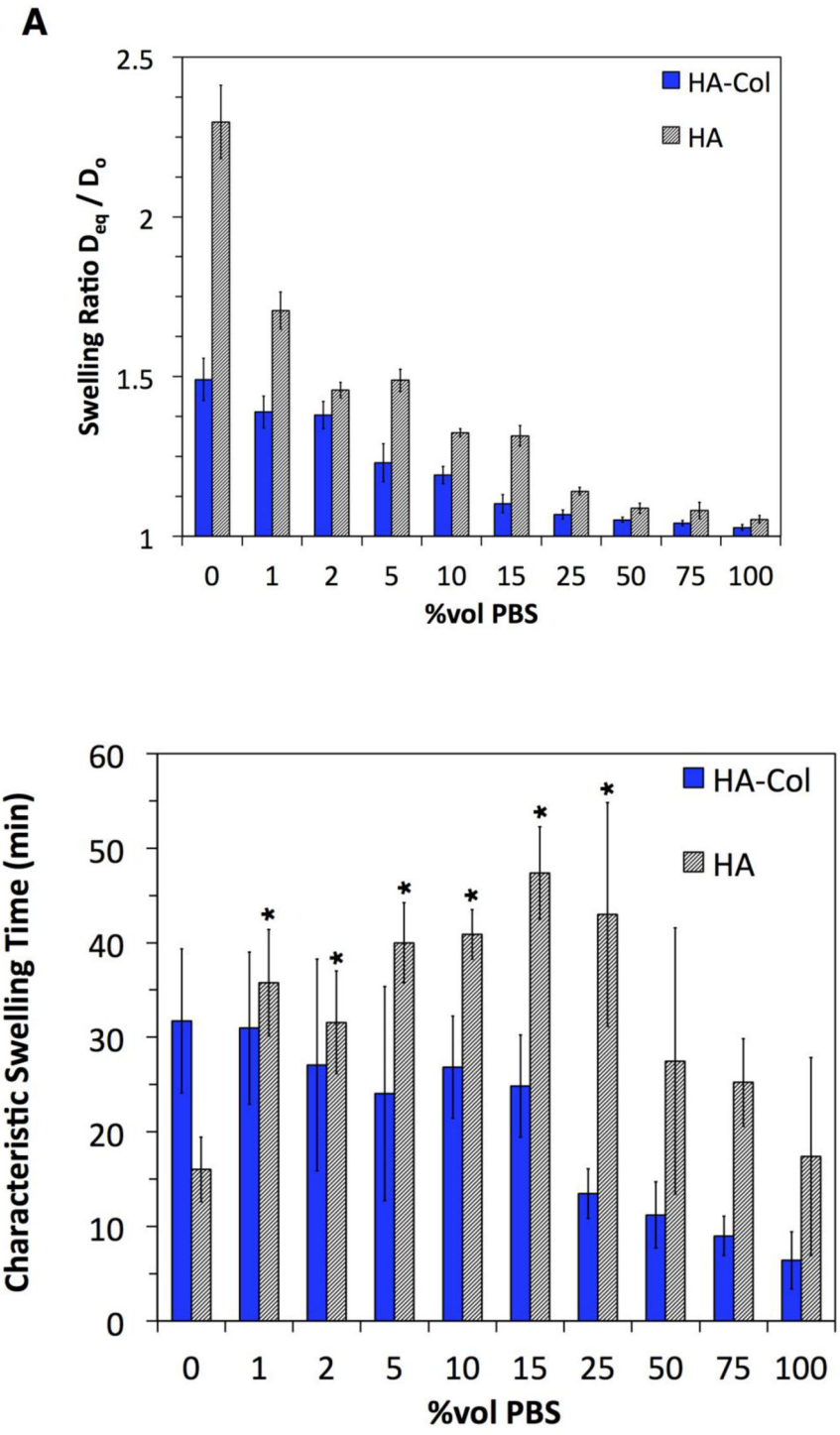

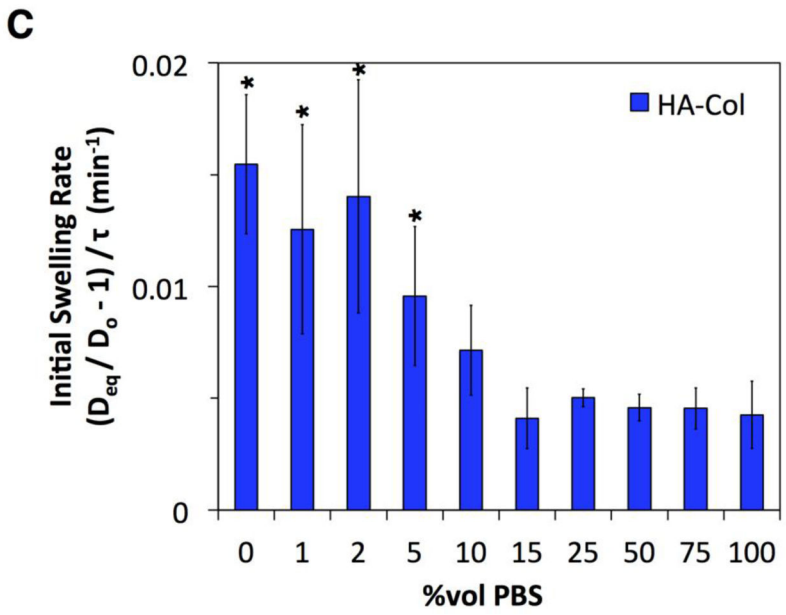

Figure 3.

(A) Equilibrium swelling ratios of HA and HA-Col gels show a decreasing trend with increasing %vol PBS. In all solutions, the HA gels swell to a larger extent than the HA-Col co-gels. (B) Average characteristic swelling times for HA-Col gels exhibit a decreasing trend with increasing PBS concentration. For the HA gels, however, swelling in 0%vol PBS show the shortest characteristic swelling time. (C) Initial swelling rate of HA-Col co-gels is faster at higher PBS concentrations. Error bars = 95% CI, n = 6 to 12. *, statistical significance at the 95% level.

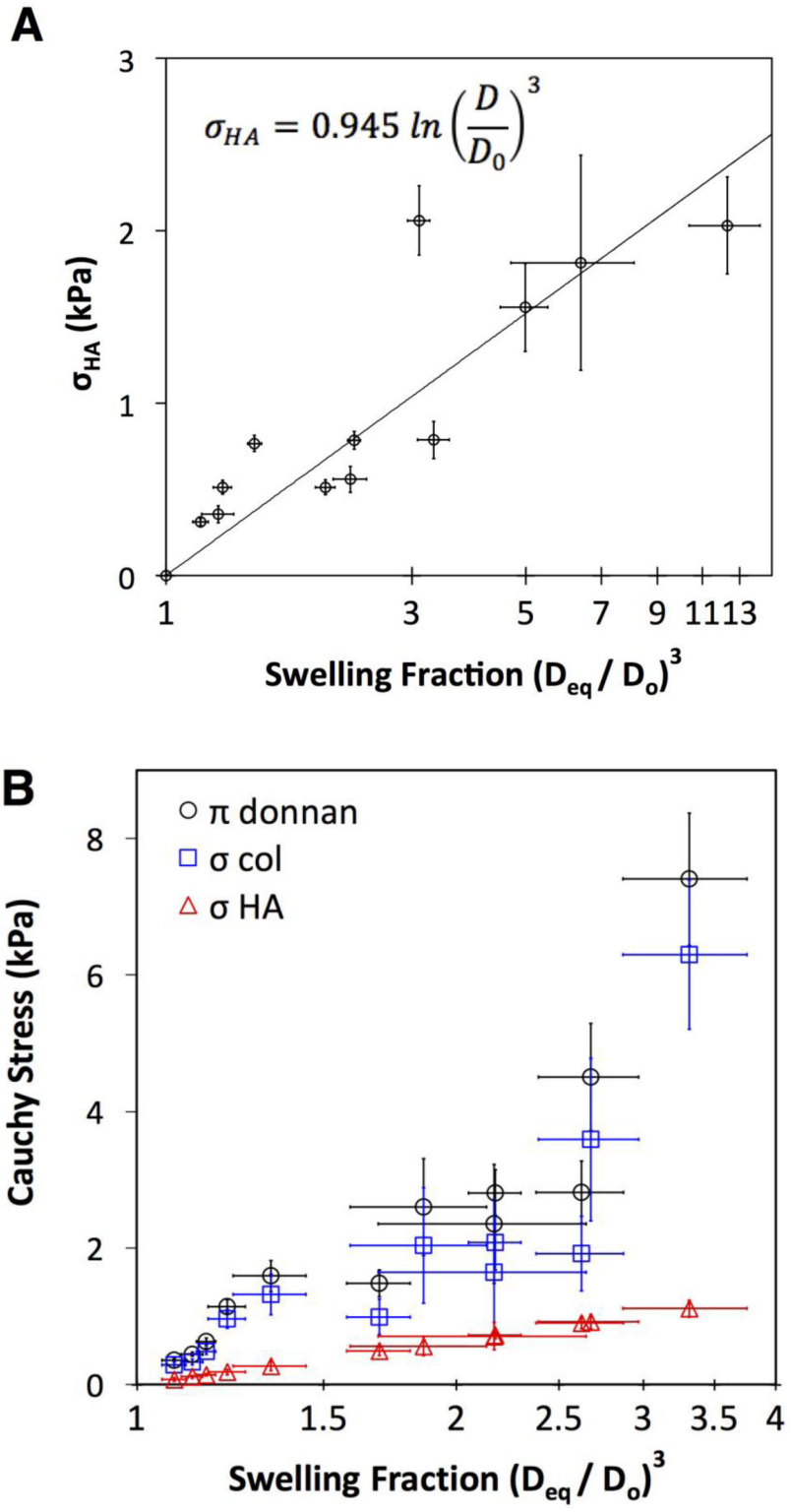

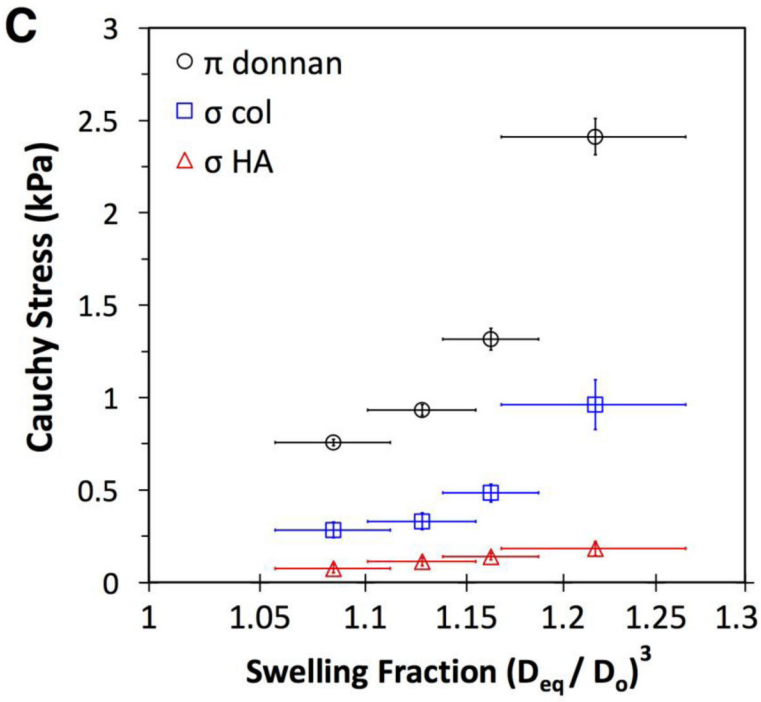

Figure 4.

(A) Average σ_{HA} from swelling of pure HA gels shows increasing stress with logarithmic swelling. $R^2 = 0.73$ (B) Relative magnitudes of σ_{HA}, π_{Donnan}, and σ_{Col} from swelling of HA-Col gels (C) Low swelling ratio region of experimental HA-Col at 100, 75, 50, 25% PBS enlarged for detail; Error bars = 95% CI, n = 6 to 12.

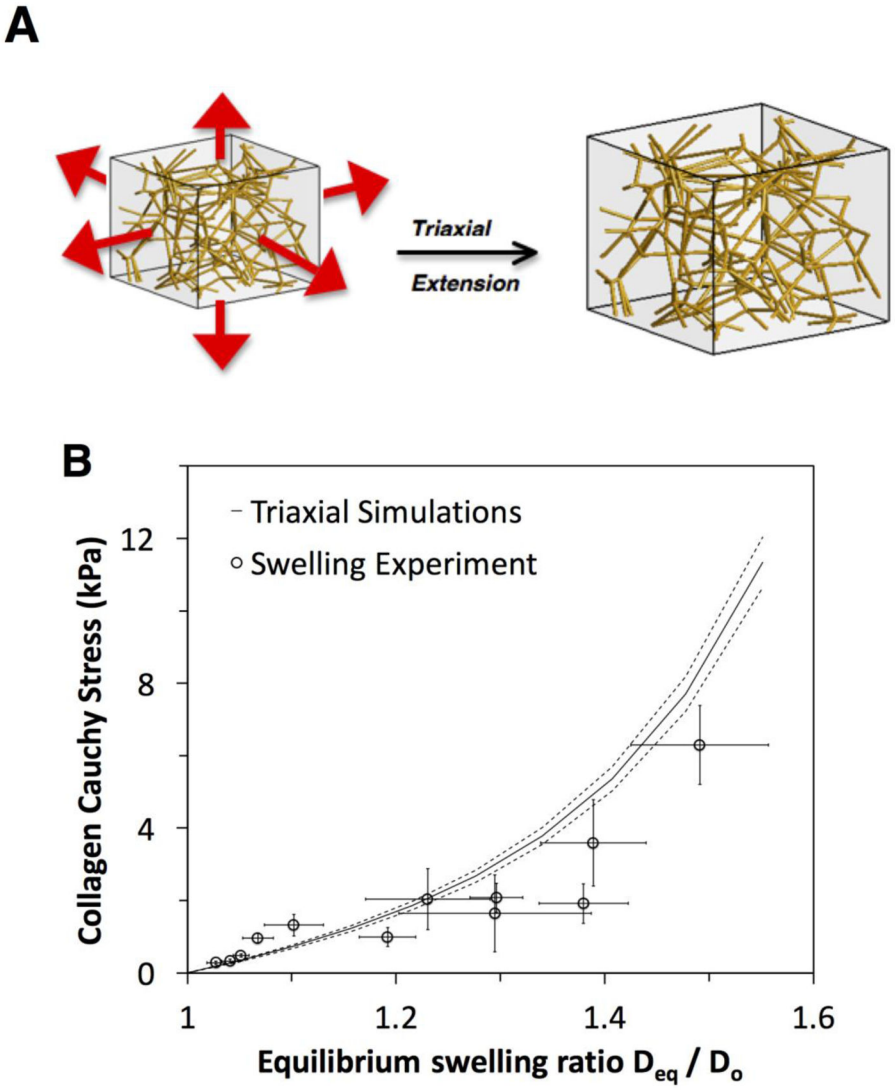

Figure 5.

(A) Simulated fiber network in triaxial extension. (B) Triaxial simulation with 95% confidence interval bounded by dotted lines. σ_{Col} calculated from experimental swelling data.